The structure of six-line ferrihydrite

E. Jansen[1,*], **A. Kyek**[2], **W. Schäfer**[1], **U. Schwertmann**[3]

[1] Mineralogisch-Petrologisches Institut, Universtät Bonn, Forschungszentrum Jülich, 52425 Jülich, Germany
[2] Physik-Department E15, Technische Universität München, 85747 Garching, Germany
[3] Lehrstuhl für Bodenkunde, Technische Universität München, 85350 Freising, Germany

Abstract. Nanocrystalline ferrihydrite (bulk formula $5Fe_2O_3 \cdot 9H_2O$) synthesized by hydrolysis of Fe(III) nitrate at 348 K was investigated by neutron diffraction at 5, 293 and 323 K. The structure is refined as a sum of a defect-free phase (space group P$\bar{3}$1c) and a defective phase (space group P3) based on earlier discussed models from X-ray diffraction results on a six-line ferrihydrite. The size of the nanoparticles was found to be 2.7 (0.8) nm. The material reveals antiferromagnetic order below $T_N = 330(20)$ K with collinear Fe spins (sequence $+ - + -$) perpendicular to the trigonal axis. The ordered moment is $3.2\,\mu_B$/Fe at 5 K.

Ferrihydrite is an Fe(III) oxyhydroxide (bulk formula: $5Fe_2O_3 \cdot 9H_2O$) of considerable importance in mineralogy and metallurgical processing. An extensive survey on this mineral has recently been published by Jambor and Dutrizac [1]. Natural ferrihydrite occurs in waters and sediments, soils, weathering crusts, and mine wastes; it is commonly formed by rapid oxidation of Fe^{2+}-containing solutions followed by hydrolysis in the presence of crystallization inhibitors [2]. In iron and steel industries, ferrihydrite occurs as a corrosion product [3].

Ferrihydrite is characterized by high dispersion, small-particle size, and poor crystallinity [4, 5]. Therefore, X-ray diffraction patterns consist of only a few broad peaks the number of which varies between 2 and 6–7. The structure was first described by Towe and Bradley in 1967 [6]. Since then, a variety of structure models have been suggested. Drits et al. [7] reported disagreements between X-ray diffractograms and the existing models. They suggested a new structure model consisting of a mixture of essentially two phases:

– a defect-free phase (space group P$\bar{3}$1c) of anionic ABACA ... close packing in which Fe atoms occupy only octahedral sites; and

– a defective phase made up of two structural fragments of the defect-free phase randomly distributed within a hexagonal super-cell.

In addition, they suggested an admixture of hematite.

The magnetic properties of ferrihydrite are also controversially discussed (see [1]). According to Murad [8] natural ferrihydrite is superparamagnetic at room temperature and remains so to temperatures as low as 23 K. Since no abrupt onset of magnetic order at a well-defined temperature occurs, superparamagnetic and magnetically ordered components should coexist over a wide temperature range. Ferrimagnetic and antiferromagnetic states are attributed to the 2-line and 6-line species, respectively [9].

Neutron diffraction, with its electron-independent nuclear scattering and its unique magnetic scattering, is considered a useful tool in obtaining complementary information with respect to both structural and magnetic properties of ferrihydrite.

1 Experiment

Six-line nanocrystalline ferrihydrite was prepared by 12-min hydrolysis of an aqueous 0.025-M $Fe(NO_3)_3$ solution at 348 K and dialysed against distilled water for 3 d [6]. The powder was contained in a cylindrical vanadium can of 7.6-mm diameter and 30-mm height. Neutron diffraction patterns were collected at 5, 293 and 323 K (see Fig. 1) using the University of Bonn powder diffractometer SV7-a at the FRJ-2 research reactor in the Forschungszentrum Jülich [10]. The neutron wavelength used was 0.1095 nm. The scattering conditions were extraordinary unfavourable due to (i) the high incoherent background occurring from the large amount of hydrogen in the compound and (ii) the large peak widths caused by the nanocrystalline nature of the ferrihydrite. An X-ray diffraction pattern (Cu K_α radiation) was taken on the same material, for comparison (Fig. 2). The neutron diffraction data analysis was based on full-pattern Rietveld refinements using the program FullProf [11].

*Corresponding author.
(Fax: +49-2461/613-012; E-mail: e.jansen@fz-juelich.de)
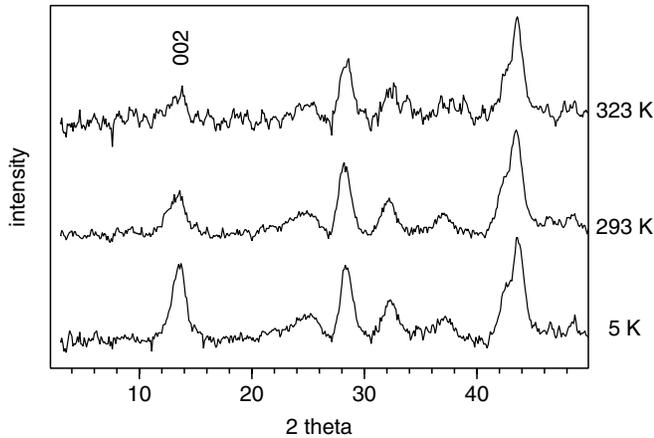
Fig. 1. Sections of the neutron diffraction patterns of ferrihydrite at 323 K (halved measuring time), 293 K and 5 K
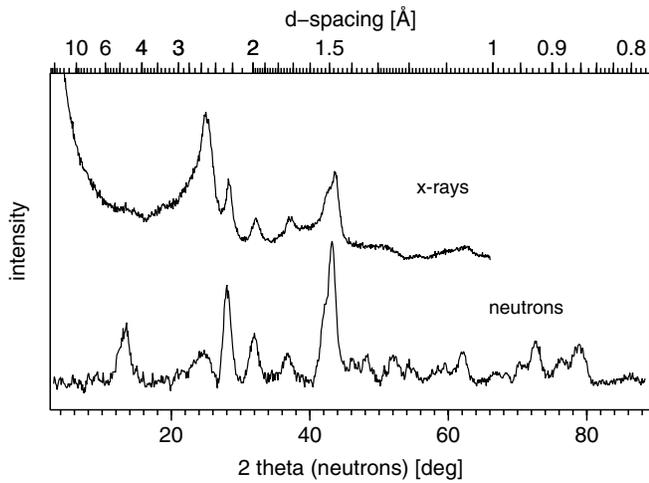
Fig. 2. Comparison of X-ray and neutron diffractograms of ferrihydrite at 293 K

2 Results

The structure analysis of the non-deuterated ferrihydrite specimen was focused on the determination of the "core structure", i.e. the iron and oxygen framework and the corresponding atomic site occupancies, by disregarding specific arrangements of hydrogen, considering the comparatively small contributions of hydrogen to the coherently scattered Bragg peaks. Accordingly, the crystal structure of ferrihydrite can best be described by a superposition of two components, as proposed by Drits et al. [7], referred to as the defect-free (f) and defective (d) phases and described in the trigonal space groups $P\bar{3}1c$ and $P3$, respectively. The room-temperature lattice constants are $a_0 = 0.2955\,(4)$ nm and $c_0 = 0.937\,(2)$ nm. The corresponding values at the measured temperatures of 5 and 323 K are $a_0 = 0.2942\,(1)$ and $0.2957\,(3)$ nm and $c_0 = 0.9361\,(9)$ and $0.946\,(2)$ nm, respectively. The layered structure of ferrihydrite is depicted in Fig. 3 indicating an ABACA sequence of OH and H for the f-phase.

The d-phase, which consists of a subunit ($c_d = c_f/2$) of the f-phase, originates from a symmetry reduction ($P\bar{3}1c \to P3$) which involves atomic site splittings and consequently a higher degree of disorder due to varying occupancies and
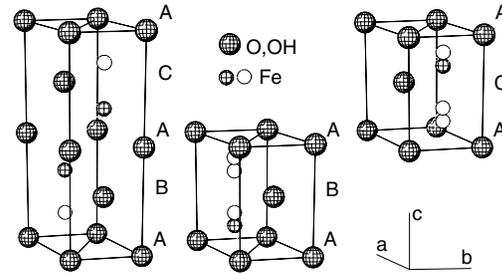
Fig. 3. The layered structure of ferrihydrite composed of a random sequence of a defect-free ABACA and two defective ABA, ACA phases. The occupation of Fe sites is indicated by *solid* and *open circles*

additional vacancies in the structure. The d-phase is modelled by random sequences of enantiomorphous ABA and ACA layers. Refined atomic positions and site occupancies in the f- and d-phases are summarized in Table 1. Figure 4 depicts the Rietveld refined diffraction pattern. The Bragg scattering contributions from the f- and d-phases which deliver R values of 13.6 and 17.0%, respectively, are separately extracted.

The nuclear Bragg scattering in the diffraction patterns is superimposed by coherent magnetic scattering due to an order of the magnetic iron spins. This is clearly visible from the first strong (002) peak when comparing the temperature-dependent neutron diffraction patterns (Fig. 1)

Table 1. Atomic position parameters x, y, z and site occupancies occ of the defect-free and defective phases

Phase	Atom	Site	x	y	z	occ
Defect-free	O,OH$_1$	2b	0	0	0	0.19(4)
	Fe	4f	1/3	2/3	0.136 (2)	0.39 (9)
	O,OH$_2$	2d	2/3	1/3	1/4	1
Defective	O,OH$_1$	1a	0	0	0	1
	Fe$_1$	1b	1/3	2/3	0.163 (3)	0.24 (2)
	Fe$_2$	1b	1/3	2/3	0.337 (3)	0.24 (2)
	O,OH$_2$	1c	2/3	1/3	1/2	1
	Fe$_3$	1b	1/3	2/3	0.663 (3)	0.24 (2)
	Fe$_4$	1b	1/3	2/3	0.837 (3)	0.24 (2)
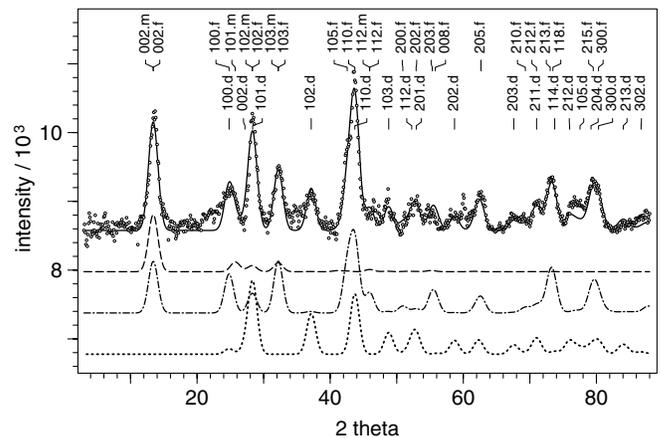
Fig. 4. Neutron diffraction pattern at 5 K with experimental data points (*dots*), the Rietveld refinement (*solid line*), and the calculated contributions of the magnetic (*dashed line*), the defect-free (*dash-dotted line*) and the defective (*dotted line*) phases

and the 5 K Rietveld refinement (Fig. 4). Determination of the magnetic structure was performed by a comparison of different spin configurations considering the octahedrally coordinated iron atoms on the 4f sites $(\frac{1}{3}, \frac{2}{3}, 0.136)$, $(\frac{1}{3}, \frac{2}{3}, 0.364)$, $(\frac{2}{3}, \frac{1}{3}, 0.636)$ and $(\frac{2}{3}, \frac{1}{3}, 0.864)$ (see Table 1). Ferromagnetic order $(+ + + +)$ as well as the antiferromagnetic spin sequences $(+ + - -)$ and $(+ - - +)$ can be excluded by appropriate magnetic structure factor calculations. The neutron measurements are in accordance with a collinear antiferromagnetic structure modelled by the $(+ - + -)$ spin configuration and magnetic moments oriented perpendicular to the trigonal axis. Refinements reveal a magnetic moment of 3.2(3) μ_B per Fe ion at 5 K. The magnetic R_{Bragg} value of the Rietveld fit is 7.6% (compare Fig. 4).

The nanocrystalline nature of the ferrihydrite specimen is evident from significant broadenings of all diffraction peaks. The quantitative analysis of the mean particle size, s, is based on the the Scherrer formula [12] $s = \lambda/(B \cos \theta)$, containing the experimental, specimen-specific peak halfwidth, B. Accordingly, a mean particle size of 2.7(8) nm was obtained for the actual ferrihydrite specimen.

3 Discussion

For the first time, neutron diffraction has been applied to structure investigations on ferrihydrite. The crystal-structure data analysis of the non-deuterated material was aimed at discriminating the various structure models published so far. The present neutron diffraction data clearly favour the ferrihydrite structure model proposed by Drits et al. [7], although the actual R_{Bragg} values of the refinement calculations are rather poor. They are, however, reasonable, keeping in mind that (i) only about 4% of the neutrons in the diffraction patterns are coherently scattered into the Bragg reflections, and (ii) the ferrihydrite structure is highly disordered. The volume percentages of the defect-free and defective phases are roughly estimated to be 50 : 50, with an error of about 10%. This estimation is based on the refined scale factors in the Rietveld refinements. The preparation of deuterated material is envisaged for a more detailed neutron study aiming at better discrimination between oxygen and hydroxyl anions. In contrast to Drits et al. [7], no admixture of hematite could be detected and, thus, does not seem to be an essential component of ferrihydrite.

Concerning the magnetic properties of ferrihydrite, our neutron diffraction data clearly reveal an ordered antiferromagnetic state. From the temperature dependence of the strongest magnetic reflection (002) (Fig. 1), the Néel temperature is extrapolated to about 330 K. An uncertainty of about ± 20 K exists because of the poor intensity situation. The onset of the antiferromagnetically ordered state already above room temperature is manifested by iron moments of 0.8 (3) and 1.6 (2) μ_B per iron ion at 323 and 293 K, respectively, according to the Rietveld analyses. The refined value of 3.2 (3) μ_B at 5 K seems reasonable for Fe ions in a compound where magnetic exchange interactions are influenced by a high degree of structural disorder. The dimension of about 2.7 nm for the coherently scattering domains as evaluated for this ferrihydrite specimen is in fairly good agreement with previous results (compare [1, 7]). The data obtained on iron concentration, particle size and magnetic moment per Fe ion result in a magnetic moment of 170 μ_B per nanoparticle. A high scatter of about 50 μ_B has to be attributed to the experimental uncertainty of about 0.8 nm in the nanoparticle size. The magnetic moment of 170 (50) μ_B per nanoparticle is in good agreement with the 210 μ_B resulting from recent investigations using a combination of Mössbauer spectroscopy and SQUID measurements [13].

References

1. J.L. Jambor, J.E. Dutrizac: Chem. Rev. **98**, 2549 (1998)
2. U. Schwertmann: In *Iron in Soils and Clay Minerals*, ed. by J.W. Stucki, B.A. Goodman, U. Schwertmann, NATO ASI Ser. **217**, 267 (1988)
3. R.M. Cornell, U. Schwertmann: *The Iron Oxides* (VCH, Weinheim 1996)
4. F.V. Chukhrov, B.B. Zvyagin, A.I. Gorshkov, L.P. Yermilova, V.V. Balashova: Int. Geol. Rev. **16**, 1131 (1973)
5. U. Schwertmann, W.R. Fischer: Geoderma **10**, 237 (1973)
6. K.M. Towe, W.F. Bradley: J. Colloid Interface Sci. **24**, 384 (1967)
7. V.A. Drits, B.A. Sakharov, A.L. Salyn, A. Manceau: Clay Miner. **28**, 185 (1993); V.A. Drits, A.I. Gorshkov, B.A. Sakharov, A.L. Salyn, A. Manseau, A.B. Sivtsov: Lithol. Miner. Resour. **1**, 68 (1995)
8. E. Murad: In *Iron in Soils and Clay Minerals*, ed. by J.W. Stucki, B.A. Goodman, U. Schwertmann. NATO ASI Ser. **217**, 309 (1988)
9. Q.A. Pankhurst, R.J. Pollard: Clays Clay Miner. **40**, 268 (1992)
10. W. Schäfer, E. Jansen, R. Skowronek, A. Kirfel: Physica B **234**, 1146 (1997)
11. J. Rodriguez-Carvajal: Physica B **192**, 55 (1993); FullProf version, 1999
12. *Intern. Tables for X-Ray Crystallography, Vol. III* (D. Reidel Publishing Company, Dordrecht 1985) p. 318
13. A. Kyek: unpublished